Alzheimer's & Dementia 12 (2016) 1250-1258

Featured Article

The effect of β-amyloid positivity on cerebral metabolism in cognitively normal seniors

Andrea C. Bozoki[a,b,c,*], Monica Zdanukiewicz[c], David C. Zhu[b,c,d], for the Alzheimer's Disease Neuroimaging Initiative[1]

[a]*Department of Neurology, Michigan State University, East Lansing, MI, USA*
[b]*Department of Radiology, Michigan State University, East Lansing, MI, USA*
[c]*Neuroscience Program, Michigan State University, East Lansing, MI, USA*
[d]*Department of Psychology, Michigan State University, East Lansing, MI, USA*

Abstract

Introduction: We evaluated the effect of cerebral amyloid-β (Aβ) deposition in cognitively normal (CN) seniors on regional metabolism of specific brain regions known to be affected by p-tau deposition.

Methods: Fluorodeoxyglucose positron emission tomography (FDG-PET), volumetric magnetic resonance imaging scans, and global amyloid standardized uptake value ratios (SUVr) were obtained for 210 CNs from the Alzheimer's Disease Neuroimaging Initiative-2 (*ADNI2*). Region of interest (ROI) extraction was used to obtain functional SUVr from six bilateral ROIs: amygdala (AM), entorhinal cortex (EC), hippocampus, lateral orbitofrontal, posterior cingulate (PC), and middle temporal gyrus. Every metabolic SUVr set was averaged and analyzed against the corresponding subject's amyloid SUVr. Correlation analyses were conducted on the full group and between *APOE* ε4-positive and *APOE* ε4-negative subgroups.

Results: The *APOE* ε4+ group exhibited significantly higher metabolism in the EC ($r = 0.270$, $P = .038$) and AM ($r = 0.267$, $P = .041$). When a significance of the difference test was conducted between the *APOE* ε4+ and *APOE* ε4-groups, these same regions remained significant: $P = .012$ and $P = .016$, respectively. By contrast, the *APOE* ε4 group displayed only the conventionally expected result of reduced regional metabolism in the PC ($r = -0.161$, $P = .048$), with higher Aβ load.

Conclusions: The effect of amyloid positivity on brain metabolism is regionally specific, and *APOE* ε4 status substantially modulates regional glucose uptake in these regions. The *APOE* ε4 allele may cause earlier emergence of clinical symptoms in AD via a mechanism that influences regional metabolic demand in specifically those regions where p-tau deposition is known to occur earliest.

Keywords: ADNI; FDG-PET; Florbetapir-PET; *APOE*; Amyloid

1. Introduction

The symptoms of Alzheimer's disease (AD) are known to be preceded by a long period of silent gradual pathological change [1,2]. Accumulation of amyloid β (Aβ) occurs in cognitively intact older people [3,4], preceding development of symptoms by several decades [5]. In addition, in developing AD, fluorodeoxyglucose positron emission tomography (FDG-PET) studies typically demonstrate cerebral hypometabolism early on, beginning in the

Disclosure: Dr. Bozoki reports receiving research support for the conduct of clinical trials from GE, Janssen AI, Pfizer, Eisai, and Toyama Pharmaceuticals. M. Zdanukiewicz, and D. Zhu report no disclosure.

[1]As such, the investigators within the Alzheimer's Disease Neuroimaging Initiative (ADNI) contributed to the design and implementation of ADNI and/or provided data but did not participate in analysis or writing of this report. A complete listing of ADNI investigators can be found in a Supplementary file labeled ADNI acknowledgments.

*Corresponding author. Tel.: +1-517-353-8122. Fax: +1-517-432-9414.
E-mail address: andrea.bozoki@ht.msu.edu

http://dx.doi.org/10.1016/j.jalz.2016.06.003
1552-5260/

posterior cingulate (PC), with the precuneus, posterior temporal and lateral parietal regions additionally becoming hypometabolic over time [6,7]. This relationship is affected by *APOE* ε4 status, with cognitively normal (CN) carriers demonstrating a significantly lower uptake of fluorodeoxyglucose (FDG)—albeit small in magnitude—in specific brain regions, including the PC, precuneus, lateral parietal, and an "AD-signature meta-ROI" [8].

It has been widely assumed that preclinical subjects exhibit normal metabolism. However, recent work suggests that high-risk asymptomatic individuals such as those with high Aβ, can present subtle regional declines in metabolism compared with those without [9–11]. More remarkably, one of these studies showed these same individuals as presenting a relatively *higher* metabolism in a different region, the medial temporal lobe [10], whereas several others found increased metabolism in medial frontal, lateral prefrontal cortices, and the anterior and/or inferior temporal regions [12,13]. The study by Yi et al. also noted that this relative elevation of metabolism was more pronounced in *APOE* ε4 carriers, regardless of cerebral amyloid load.

Of the regions mentioned as showing greater FDG uptake in persons with high cerebral Aβ levels, the medial temporal lobe is most relevant, as it is the earliest cortical region to develop the other characteristic pathology of AD, neurofibrillary tangles (NFTs) [14,15]. The trajectory of involvement begins in the entorhinal cortex (EC), spreads to adjacent amygdala and/or hippocampus (AM/HIPP) followed by other portions of the limbic system and eventually involves neocortical regions. Haiko and Eva Braak termed involvement of these regions as stages I, II, III/IV, and V/VI, respectively, with stages I, II, and III still compatible with normal cognition. In conjunction with these pathologic data, there is a large body of work supporting the close relationship of elevated cerebrospinal fluid (CSF) tau levels with cognitive decline, abnormal levels of which occur far closer in time to the onset of clinically apparent symptoms than the appearance of cerebral Aβ [16,17]. However, it is still unknown whether CSF tau levels increase substantially at Braak & Braak stages I, II, or only III.

We hypothesized that, early in the course of NFT deposition, clinically healthy individuals with a high burden of cerebral amyloid would demonstrate subtle regional increases in metabolism in those medial temporal regions corresponding to Braak stages I and II (and possibly III), correlating with progressive involvement of these regions by NFT-laden neurons at a stage when, despite cell death, many neurons in these regions were still relatively healthy and could thus keep up with higher metabolic demand. Furthermore, we hypothesized that CSF p-tau levels would correlate with the elevated metabolism in these same regions if we were capturing individuals who were already undergoing neuronal cell death, when levels of extracellular, soluble p-tau are high enough to be detected by assays. Finally, given the younger age of onset and more rapid clinical decline in *APOE* ε4+ patients, we explored the possibility of a differential relationship between genotypes and the emergence of higher metabolic demands during the preclinical phase of AD development.

2. Methods

2.1. Subjects

Data used in the preparation of this article were obtained from the Alzheimer's Disease Neuroimaging Initiative (ADNI) database (adni.loni.usc.edu; see Supplementary Data 1). Our image data consisted of T1-weighted high-resolution volumetric magnetic resonance and FDG-PET images of healthy controls downloaded from the ADNI database over the course of the study, the latest in August 2014 (http://adni.loni.usc.edu). Additional data used for the study included subject *APOE* ε4 status, CSF p-tau, and global amyloid standardized uptake value ratios (SUVr). The individual ADNI subject identifiers used in this study can be found in Supplementary Data 2.

2.2. Standard protocol approvals, registrations, and patient consents

The ADNI was approved by the institutional review board at each site and was compliant with the Health Insurance Portability and Accountability Act. Written consent was obtained from all participants.

2.3. Magnetic resonance image acquisition and preprocessing

All participants who were newly enrolled in ADNI2 were scanned using a high-resolution 3T volumetric magnetic resonance imaging (vMRI) protocol during screening (http://adni.loni.usc.edu/methods/mri-analysis/mri-acquisition). Images downloaded for the study had undergone the maximum level of correction (i.e., warping, intensity correction, and scaling for gradient drift using the phantom data) and were identified with "N3" and "scaled" in the file name. Further information can be found in the ADNI2 Alzheimer's Disease Neuroimaging Initiative 3T MRI Technical Procedures Manual.

2.4. Positron emission tomography (PET) image acquisition and preprocessing

The ADNI acquires florbetapir (AV45) and FDG-PET scans from all newly enrolled participants on two separate days. Scans may be performed in any order, but both must be completed within 2 weeks of the in-clinic assessments at baseline. FDG-PET scans downloaded for this study had

undergone the maximum level of correction (i.e., coregistered dynamic, averaged, standardized image and voxel size, and uniform resolution). Of note, ADNI FDG-PET data are normalized to a global SUVr: an averaged image is generated from the six individual coregistered frames and then intensity normalized using a subject-specific mask so that the average of voxels within the mask is exactly 1. This process, and a subsequent image smoothing step, is done to make comparison of data from different scanners more straightforward. Further details on ADNI PET methods can be found at *adni.loni.usc.edu/data-samples/pet/*.

AV45-PET scans were not downloaded for direct analysis in the study. These scans were analyzed by the University of Utah. We chose to use a mean amyloid SUVr value derived from temporal and parietal association cortex amyloid made available on the ADNI site (UU-PET Analysis, v.2014-1-31) under the variable name "AVEASSOC." These AV45 scans were normalized to cerebellum. A complete description of their method for deriving these values can be found in *UU–PET Analysis Methods* located at adni.loni.usc.edu.

2.5. MR and PET image postprocessing and coregistration

Analysis of Functional NeuroImages (AFNI; http://afni.nimh.nih.gov/) was used for all post-processing conducted to coregister vMR images to their respective FDG scans. All images were refit to original space, centered, and aligned to their partnering data set. Volumetric scans that were acquired obliquely were reoriented and resliced to cardinal coordinate space before centering and realignment; similar steps were taken for respective PET images. Visual inspection was used to evaluate individual coregistration to ensure accuracy.

2.6. ROI creation and SUVr acquisition

FreeSurfer was used for image segmentation and the creation of anatomical ROIs [18]. After reconstruction and segmentation, we extracted six of these bilaterally parcellated areas for use as ROI masks in the glucose uptake analysis: EC, AM, HIPP, PC, middle temporal gyrus (MTG), and lateral orbitofrontal (LOF) gyrus. AFNI was then used to obtain the SUVr for each ROI from the coregistered FDG-PET. All coregistered ROI masks were visually inspected and corrected where necessary to ensure accurate data extraction.

2.7. Genetic and biomarker acquisition

Our study included subject *APOE* ε4 status acquired from Merged ADNI v. 2013-04-29, CSF p-tau from UPENN—CSF Biomarkers v. 2013-10-31, and global amyloid SUVr from UU—PET Analysis v. 2014-01-31.

2.8. Statistical analysis

Analyses were done with SPSS 22 (SPSS, Inc., Chicago, IL, USA). Independent *t*-tests were performed for all demographic variables. FDG-SUVr values from the two hemispheres were averaged for each subject before statistical analysis, yielding a single mean value per ROI. The distribution of glucose uptake values in all six examined brain regions was normally distributed; thus, *Pearson correlation* was performed to examine the relationship between amyloid burden and ROI glucose uptake, as well as the relationship between p-tau and ROI glucose uptake. A *significance of difference between two correlations test* [19,20] was then used to directly compare *APOE* ε4+ and *APOE* ε4-groups for each of the six bilateral ROIs. Significance was based on a two-tailed analysis with $P < .05$. Stepwise regression was conducted to determine if age, gender, or level of education acted as confounding factors in the *APOE* ε4 group analyses.

2.9. Subject disposition and demographic characteristics

A total of 211 CN individuals matched the necessary inclusion criteria. The mean age and education level for the whole group was 74.2 (6.3) and 16.6 (2.5), respectively. There were 104 men in the pool. Age, education, and gender were not significantly different between groups. Of the total, 152 had no *APOE* ε4 allele, 53 had one, and six had two alleles. *APOE* ε4 values of 0 were categorized as the negative group, and values of 1 and 2 were combined to form the positive group. Overall, 165 of 211 subjects had CSF p-tau values recorded: 120 of 152 in the *APOE* ε4-sample and 45 of 59 *APOE* ε4+ (Table 1).

3. Results

3.1. SUVr correlation analysis

Although there were no significant associations between Aβ deposition and FDG-SUVr when the entire CN group was examined together, the *APOE* ε4+ subgroup exhibited significantly higher rates of metabolism in both the EC ($r = 0.270$, $P = .038$) and AM ($r = 0.267$, $P = .041$) with increasing amyloid load, and these two regions remained significant when a significance of the difference test was conducted between the *APOE* ε4+ and *APOE* ε4-subjects (EC $Z = 2.506$, $P = .012$ and AM $Z = 2.407$, $P = .016$, respectively). *APOE* ε4-subjects showed a negative correlation between Aβ deposition and FDG-SUVr in the PC:

Table 1
Subject disposition and demographic characteristics

Variable	n = 211	*APOE* ε4−	*APOE* ε4+	*P*
Age, y (standard deviation [SD])	74.2 (6.3)	74.6 (6.0)	73.1 (7.0)	.13
Female, n (%)	107 (50.7)	74 (49)	33 (55.9)	.37
Education, y (SD)	16.6 (2.5)	16.7 (2.5)	16.2 (2.6)	.19

r = −0.161, $P = .048$, but this difference was no longer significant when the *APOE* ε4+ and ε4− groups were directly compared using the significance of the difference test. We did not correct for multiple comparisons because our a priori hypothesis was such that we expected to see differences only in ROIs affected at preclinical Braak & Braak stages and included later-stage ROIs primarily to serve as control regions (Table 2 and Fig. 1).

3.2. P-tau correlation analysis

Consistent with prior reports [21,22], CSF p-tau levels correlated strongly with amyloid burden in this CN group (r = 0.267; $P = .001$). This relationship was also true for *APOE* ε4 considered separately (r = 0.239; $P = .009$), although the smaller group size of *APOE* ε4+ who had CSF results did not demonstrate this same relationship (r = 0.281; $P = .061$; Table 3 and Fig. 2).

As with the FDG–amyloid relationship, there were no significant findings in the total sample between FDG-SUVr and CSF p-tau levels in any of our examined regions. In the *APOE* ε4+ subgroup; however, we did find significant relationships between p-tau and EC (r = 0.307, $P = .040$), p-tau and LOF (r = 0.322; $P = .031$), and p-tau and MTG (r = 0.378; $P = .011$). There were no significant findings in any examined ROI for the *APOE* ε4-subgroup. Unlike our examination of the FDG–amyloid relationship, the p-tau regional findings did not survive direct comparison using the significance of differences test.

4. Discussion

Our findings indicate that: (1) the effect of amyloid positivity on brain metabolism is regionally specific: medial temporal regions (EC and AM, although not HIPP), which are the first to develop p-tau pathology, show greater effects than temporal neocortex, orbitofrontal regions or PC gyrus, which only accrue substantive numbers of NFTs during clinically symptomatic disease; and (2) *APOE* ε4 status substantially modulates regional glucose uptake in these regions, such that greater amyloid load is not correlated with regional metabolism in *APOE* ε4-individuals, but a positive correlation with metabolism is seen in these same regions in the *APOE* ε4+ group. Intriguingly, several groups have reported that this same phenomenon is even more robustly present in individuals with Down syndrome (DS) before the development of AD [23,24]. The authors, based on both direct pathologic examination of their DS subjects, whose age range was between 5 months and 67 years, along with examinations of a rodent model of EC tau pathology, hypothesize a compensatory synaptic and neurite outgrowth in response to the evolving p-tau protein pathology. If *APOE* ε4 positivity increases the vigor of this compensatory metabolic response similar to having a third copy of the APP gene (and/or a homologue of the β-site APP cleaving enzyme which is also located on c21), it suggests one mechanism by which the *APOE* ε4 allele may cause earlier emergence of clinical symptoms in AD. It also suggests that, for these individuals, a therapeutic approach that provides for the increased energy needs of these neurons may help protect this vulnerable population and provides an explanation for the differential effects of certain antiamyloid therapies based on *APOE* status. A better understanding of prodromal metabolic derangements in key brain regions may allow different therapeutic options to be targeted to the patient population and stage of pathology at which they can still affect a change.

Our examination of the relationship between amyloid and p-tau in this CN population was somewhat more complicated. Although we demonstrated a strong positive correlation between global amyloid burden and CSF p-tau concentration (as have many other groups) in the overall group and the *APOE* ε4- subgroup, this relationship did

Table 2
Correlation of amyloid burden with p-tau concentration and FDG-PET metabolism

Group	p-tau	EC SUVr	AM SUVr	HIPP SUVr	LOF SUVr	MTG SUVr	PC SUVr
Whole group (N = 211; p-tau N = 165)							
Pearson	0.267	0.025	0.006	−0.014	−0.109	−0.040	−0.097
P value	*.001*	.722	.929	.835	.114	.566	.160
APOE ε4-negative group (N = 152; p-tau N = 120)							
Pearson	0.239	−0.115	−0.103	−0.083	−0.161	−0.098	−0.059
P value	*.009*	.158	.207	.312	*.048*	.230	.469
APOE ε4-positive group (N = 59; p-tau N = 45)							
Pearson	0.281	0.270	0.267	0.168	0.096	0.155	−0.200
P value	.061	*.038*	*.041*	.204	.471	.240	.128
Significance of the difference between *APOE* ε4 groups							
Z-score	−0.250	−2.506	−2.407	−1.609	−1.650	−1.628	0.915
P value	.802	*.012*	*.016*	.108	.099	.104	.360

Abbreviations: AM, amygdala; EC, entorhinal cortex; FDG-PET, fluorodeoxyglucose positron emission tomography; HIPP, hippocampus; LOF, lateral orbitofrontal; MTG, medial temporal gyrus; PC, posterior cingulate; SUVr, standardized uptake value ratios.

NOTE. Differences with *P* values <.05 are indicated in italic.

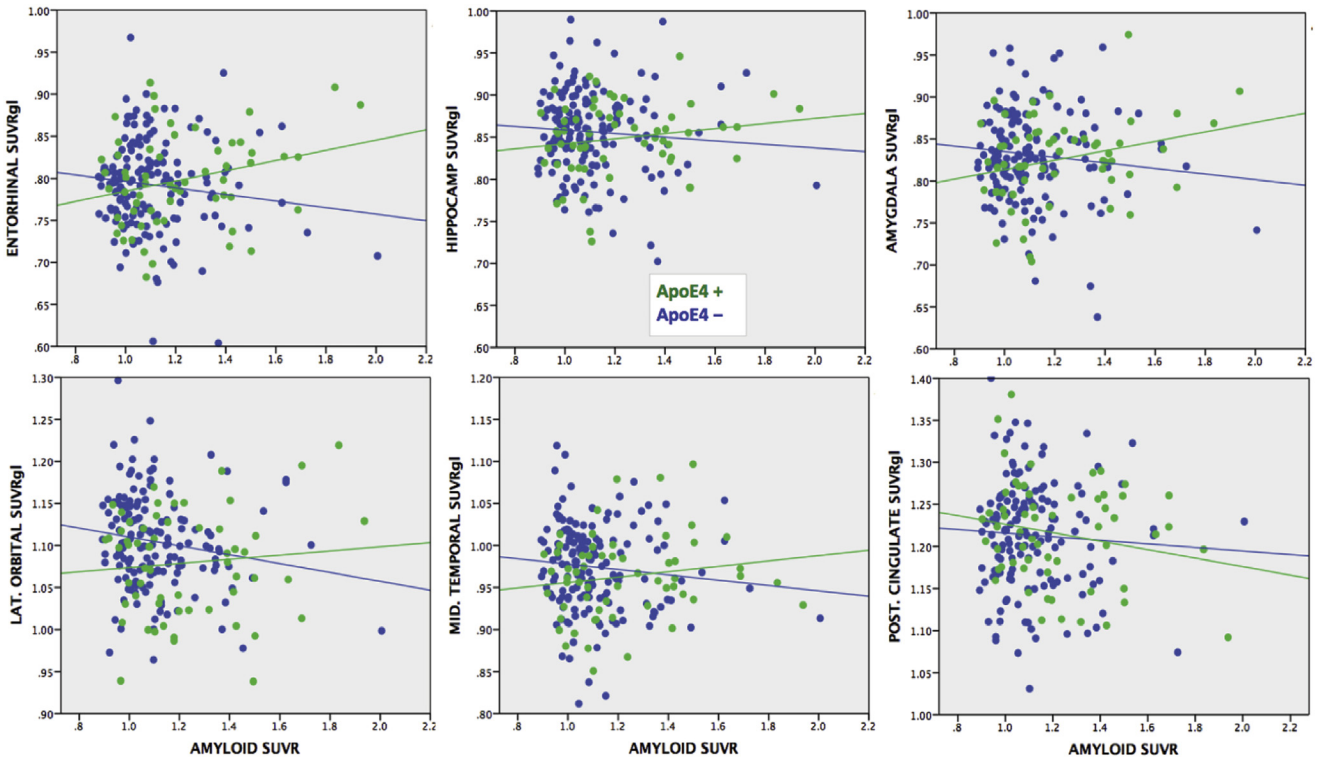

Fig. 1. Global amyloid concentration versus regional glucose metabolism for all six ROIs. Scatterplots for each of the six ROIs, with global (association cortices) amyloid SUVr for each subject on the X axis and ROI-specific glucose SUVr on the Y axis. The regression line is drawn separately for *APOE* ε4-positive and ApoE e4-negative groups for ease of comparison. Abbreviations: ROI, region of interest; SUVr, standard uptake value ratio.

not extend to the *APOE* ε4+ group, likely due to inadequate power. In addition, we found a relationship between p-tau and regional FDG-PET metabolism in the *APOE* ε4+ group but failed to replicate the regional specificity of this relationship in the predicted manner. That is, there was a correlation of CSF p-tau level with metabolism in EC, but not with AM or HIPP, and there was a relationship with metabolism in LOF and neocortical regions, which are typically less involved with NFT at preclinical stages of AD. The smaller sample size for CSF data combined with the challenge of quantitative p-tau analysis by assay [25] may have contributed to these results.

We set out to systematically examine a set of brain regions that capture the presumed trajectory of tau-tangle spread within the cortex, which begins first in the transentorhinal region of the EC and gradually spreads to encompass, first, AM and HIPP, then adjacent areas of neotemporal and orbitofrontal cortex, and finally, more distant neocortical regions including the PC [14,15,26]. This evolution of NFT pathology occurs in parallel with a similar progression of Aβ deposition, although the latter begins in a spatially widespread way, with simultaneous appearance of plaques in most neocortical association regions during a stage now termed Thal phase 1 [15,27]. We did this study to gain a better understanding of the relationship between progressive amyloid accumulation and NFT-based neuronal damage. We assumed, given recent work [5,22], that Aβ deposition would be the earliest event signaling the divergence of a healthy brain onto the path of evolving AD, understanding that there can be a period of more than 20 years where amyloid accumulates "silently" in a CN individual [2], but that at some point *later than the start of Aβ accumulation*, the process of NFT creation and spread begins—most likely due to an indirect mechanism because amyloid is never seen within EC at Thal phase I [27]. This last is actually a very important point when examining regional brain metabolism: any differences seen on FDG-PET in the EC, AM, and HIPP in amyloid + CN are *not* due to direct consequences of amyloid toxicity during Thal phase I.

Most intriguingly, our main finding, of increasing metabolism with increasing amyloid load in early NFT-associated brain regions, occurred only in the *APOE* ε4+ subgroup. This is consistent with the findings of several other recent studies examining the effects of amyloid deposition on brain metabolism. A study by Scheef et al. [10] found increased metabolism in right parahippocampal gyrus and HIPP in subjective memory impaired group compared with controls (regardless of *APOE* ε4 status, which was ∼1/3 of their sample). More recently, Oh et al. [12] examined 52 healthy seniors using PiB-PET, FDG-PET, and structural magnetic resonance imaging. Their findings suggested that CN older adults with greater amyloid deposition are relatively hypermetabolic in frontal and parietal brain

Table 3
Correlation of p-tau with FDG-PET metabolism

Group	EC SUVr	AM SUVr	HIPP SUVr	LOF SUVr	MTG SUVr	PC SUVr
Whole group (N = 165)						
Pearson	0.080	0.144	0.007	0.079	0.134	−0.038
P value	.306	.065	.933	.311	.087	.626
APOE ε4-negative group (N = 120)						
Pearson	−0.002	0.104	−0.036	0.015	0.058	−0.043
P value	.987	.257	.698	.868	.532	.643
APOE ε4-positive group (N = 45)						
Pearson	0.307	0.253	0.165	0.322	0.378	−0.044
P value	*.040*	.094	.279	*.031*	*.011*	.775
Significance of the difference between *APOE* ε4 groups						
Z-Score	−1.775	−0.857	−1.126	−1.773	−1.889	0.006
P value	.076	.391	.260	.076	.059	.996

Abbreviations: AM, amygdala; EC, entorhinal cortex; FDG-PET, fluorodeoxyglucose positron emission tomography; HIPP, hippocampus; LOF, lateral orbitofrontal; MTG, medial temporal gyrus; PC, posterior cingulate; SUVr, standardized uptake value ratios.

NOTE. Differences with *P* values <.05 indicated in italic.

regions while undergoing gray matter volume loss in overlapping brain regions. Finally, Yi et al. [13] found that *APOE* ε4+ CN had hypermetabolism relative to their *APOE* ε4-counterparts, although in medial frontal and anterior temporal regions.

Taken together, these results suggest that this genotype modulates the appearance of clinical symptoms by causing a more aggressive, metabolically vigorous response in NFT-evolving regions. Hypermetabolism on FDG-PET can be seen due to mechanisms that increase energy needs of any brain cellular component, including astrocytes, oligodendrocytes, or even indicating the presence of substantial neuroinflammatory cells (activated microglia); thus, it is unclear whether the observed phenomenon has a neuronal

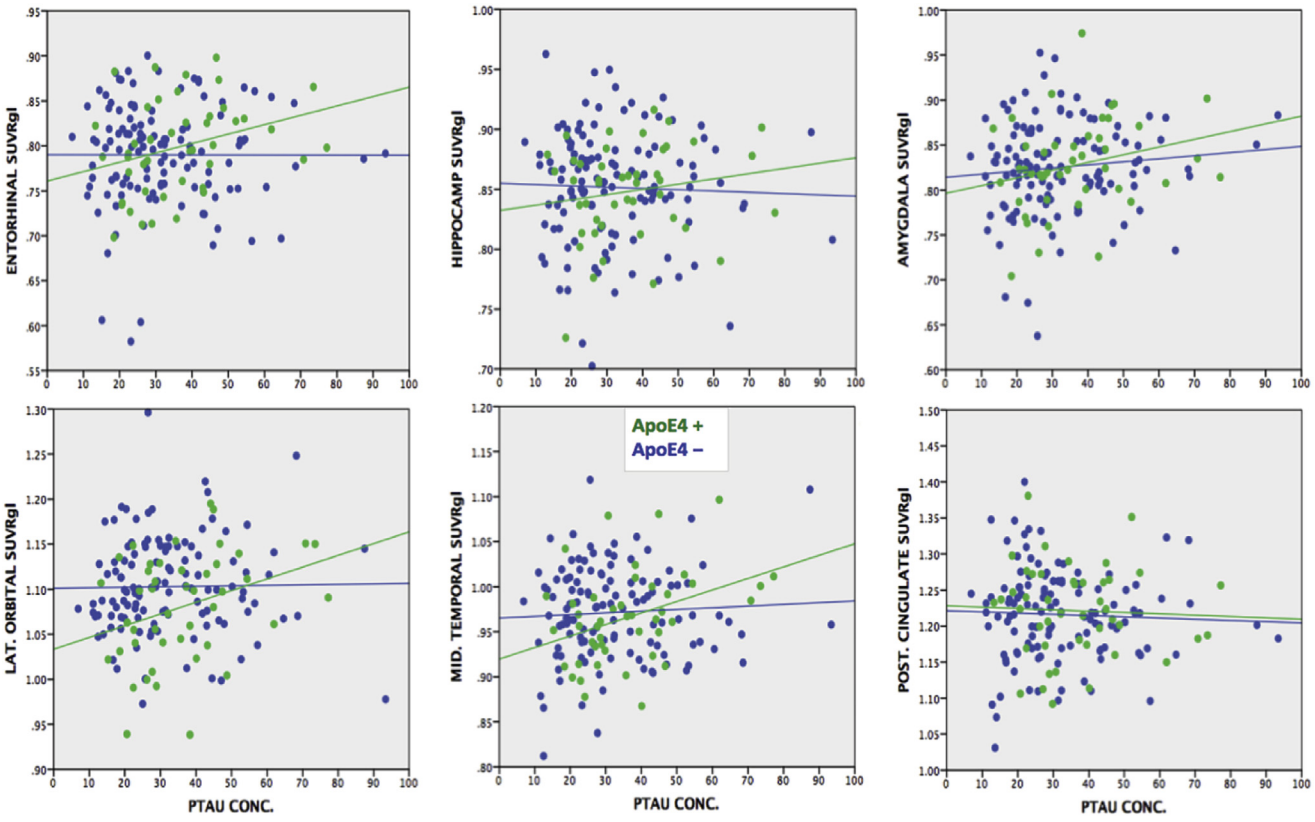

Fig. 2. CSF phospho-tau concentration versus regional glucose metabolism for all six ROIs. Scatterplots for each of the six ROIs, with CSF phosphor-tau concentration for each subject on the X axis and ROI-specific glucose SUVr on the Y axis. The regression line is drawn separately for *APOE* ε4-positive and *APOE* ε4-negative groups for ease of comparison. Abbreviations: ROI, region of interest; SUVr, standard uptake value ratio.

origin, although most of the known adverse effects of *APOE*4 protein affect neurons (by both AB-specific [28,29] and non–AB-dependent mechanisms [30–33]), with some evidence pointing toward direct toxicity of *APOE* ε4 fragments on NFT formation [34,35]. Thus, our findings point toward a compensatory response in regions of NFT formation, either due to increased synapse development and connectivity, or to a stage of sustained or recurrent neuronal excitation ("hyperexcitability") occurring during NFT production. Either of these events may occur more vigorously in *APOE* ε4+ individuals who experience an earlier and more rapidly progressive form of AD.

It must be acknowledged that not all groups who have examined the relationship between Aβ and FDG metabolism in CN have found hypermetabolic brain regions, although substantial methodologic differences may account for their lack in this area. For example, a 2012 study found no significant relationship at all between amyloid deposition and FDG metabolism. Their use of a single "metaROI" (the mean FDG uptake in a set of ROIs including R/L inferior temporal, lateral parietal, and PCC, relative to pons/cerebellum) in a group of 126 CNs taken from ADNI [36]. It is therefore unsurprising that they found no individual regional effects, as any foci of elevated metabolism would have been lost when averaged with multiple larger brain regions in which eumetabolism or hypometabolism was observed. Another article published that same year [37] noted that an "AD signature" of FDG-PET regional hypometabolism might not actually be strongly tied to amyloid deposition, in describing a group of neurodegeneration+ (by either FDG-PET or vMRI), amyloid—individuals they termed "SNAP." This study also used a composite ROI approach (comprised of the angular gyrus, PC, and inferior temporal cortical ROIs normalized to pons and cerebellar vermis), which precludes analysis of specific target brain regions. Finally, a recent study of the large Mayo Clinic Aging cohort (600 CN elders) found no hypermetabolism in any examined brain region and no relationship between *APOE* status and brain metabolism in a group of 600 CN subjects [11]. However, they did not perform the analysis done in this article; that is, they did not compare the range of amyloid positivity between *APOE* ε4+ and *APOE* ε4−groups, they examined only the mean FDG value present at a fixed PiB SUVr of 1.4. Thus, they missed finding the possible relationship between change in regional metabolism and change in PiB SUVr.

In light of the above, we note that there are undoubtedly multiple different causes of hypometabolism, which is a nonspecific sign of neuronal injury. It can be seen due to late-stage/severe amyloid deposition local to those brain regions [36,38]; it may also be seen on a "disconnection" basis in earlier disease states, where it may also be at sites removed from the heaviest burden of amyloid deposition (possibly in neuronal projection areas) [39–41]. This multiple-cause problem may be at the root of why different research groups see the hypometabolism in different brain regions.

Although the causes of hypometabolism are multiple, hypermetabolism strongly implies an increase in local cellular energy needs. Hyperphosphorylation requires adenosine triphosphate (ATP) and vigorous hyperphosphorylation would induce a relative hypermetabolic state in these cells while they were still relatively healthy and could "keep up" with the higher metabolic demand.

The aforementioned hypothesis explains why many other authors have failed to find elevated metabolism in FDG-PET studies of high-risk normal individuals; they are looking in the wrong place. By choosing to examine either brain regions with early and/or heavy amyloid load, or by averaging the metabolism across large portions of the brain, they have missed the relatively subtle signal present in the limited brain regions affected by hyperphosphorylation in preclinical AD. And in fact, this signal is only present in *APOE* ε4+ individuals, (possibly because of the higher rate of pathologic p-tau formation), so, it would also be missed by studies that fail to examine that subgroup specifically. This observation begs the question of whether *APOE* ε4− but high-risk groups (e.g., those with a mutation in the APP gene) would demonstrate this same early relative hypermetabolism in p-tau–susceptible regions.

4.1. Limitations

It is currently unclear whether tau tangles appear in substantial numbers beyond the EC during Thal phase 2 (amyloid in the EC and HIPP CA1 regions), or if phase 3 (amyloid in other parts of the HIPP, plus the deep gray nuclei) is required for this event. It is also unclear what Thal phase is the earliest to come up as "amyloid positive" on a florbetapir scan. These uncertainties regarding the relative ordering of pathologic stages between tau and B-amyloid trajectories argue for additional analyses on large brain bank populations and would help substantially in understanding the relationship (and possible causal linkages) between the two types of pathologic protein accumulation. In addition, as a cross-sectional retrospective study, our analysis captures only a "snapshot in time." It does not address the evolution of relatively increasing or decreasing metabolism of brain regions in response to progressive amyloid accumulation (and, presumably, to accumulating NFT-mediated neuronal injury). As discussed, timing may be critical in the manifestation of hypermetabolism and hypometabolism, with a preponderance of different ongoing brain insults leading to a different FDG-PET "phenotype" during the long prodromal AD phase at any given time. It will take further data collection and development of more robust methods for getting around test–retest variability in PET imaging before a nuanced understanding

of the trajectory of metabolic change can be examined accurately and merged with the aforementioned neuropathologic correlation to identify which mechanisms of brain damage lead to hypermetabolism and hypometabolism, respectively.

Acknowledgments

The authors thank Dr. Paul Beach, for assistance with data analysis; Michigan State University's High Performance Computer Center for providing storage space and computing resources.
Data collection and sharing for this project was funded by the Alzheimer's Disease Neuroimaging Initiative (ADNI; National Institutes of Health Grant U01 AG024904) and DOD ADNI (Department of Defense award number W81XWH-12-2-0012). ADNI is funded by the National Institute on Aging, the National Institute of Biomedical Imaging and Bioengineering, and through generous contributions from the following: Alzheimer's Association; Alzheimer's Drug Discovery Foundation; Araclon Biotech; BioClinica, Inc.; Biogen Idec Inc.; Bristol-Myers Squibb Company; Eisai Inc.; Elan Pharmaceuticals, Inc.; Eli Lilly and Company; EuroImmun; F. Hoffmann-La Roche Ltd and its affiliated company Genentech, Inc.; Fujirebio; GE Healthcare;; IXICO Ltd.; Janssen Alzheimer Immunotherapy Research & Development, LLC.; Johnson & Johnson Pharmaceutical Research & Development LLC.; Medpace, Inc.; Merck & Co., Inc.; Meso Scale Diagnostics, LLC.; NeuroRx Research; Neurotrack Technologies; Novartis Pharmaceuticals Corporation; Pfizer Inc.; Piramal Imaging; Servier; Synarc Inc.; and Takeda Pharmaceutical Company. The Canadian Institutes of Rev December 5, 2013 Health Research is providing funds to support ADNI clinical sites in Canada. Private sector contributions are facilitated by the Foundation for the National Institutes of Health (www.fnih.org). The grantee organization is the Northern California Institute for Research and Education, and the study is coordinated by the Alzheimer's Disease Cooperative Study at the University of California, San Diego. ADNI data are disseminated by the Laboratory for Neuroimaging at the University of Southern California.
Authors' contributions: A.C.B. contributed to conceptual framework, data analysis, and article writing. M.Z. contributed to MR and PET data processing, statistical analysis, and article writing. D.Z. contributed to MR and PET data processing, article review, and editing.
Study funding: No targeted funding was reported.

Supplementary data

Supplementary data related to this article can be found at http://dx.doi.org/10.1016/j.jalz.2016.06.003.

RESEARCH IN CONTEXT

1. Systematic review: The authors reviewed existing studies of neuronal metabolism as examined by fluorodeoxyglucose positron emission tomography (FDG-PET), in cognitively normal seniors at risk for developing AD and nondemented Down's patients. Reports of elevated regional metabolism were contrasted with those reporting unchanged or hypometabolism to formulate a hypothesis that elevated metabolism could be related to neuronal regions affected by increased tau phosphorylation.
2. Interpretation: We found regional elevations of FDG-PET metabolism in the specific regions known to harbor the early emergence of tau-mediated damage in individuals with prodromal AD. This metabolic activity was specific to *APOE* ε4+ individuals.
3. Future directions: Our results need to be validated in a longitudinal study of metabolic change over time. The eventual development of clinical AD in only those individuals showing sequential rising, then falling metabolism in tau-affected regions after Braak stages, would provide a means of identifying preclinical AD with greater certainty in amyloid-positive individuals.

References

[1] Price JL, Morris JC. Tangles and plaques in nondemented aging and "preclinical" Alzheimer's disease. Ann Neurol 1999;45:358–68.
[2] Bateman RJ, Xiong C, Benzinger TLS, Fagan AM, Goate A, Fox NC, et al. Clinical and biomarker changes in dominantly inherited Alzheimer's disease. N Engl J Med 2012;367:795–804.
[3] Mintun MA, LaRossa GN, Sheline YI, Dence CS, Lee SY, Mach RH, et al. [11C]PIB in a nondemented population: potential antecedent marker of Alzheimer disease. Neurology 2006;67:446–52.
[4] Aizenstein HJ, Nebes RD, Saxton JA, Price JC, Mathis CA, Tsopelas ND, et al. Frequent amyloid deposition without significant cognitive impairment among the elderly. Arch Neurol 2008;65:1509.
[5] Jack CR Jr, Albert MS, Knopman DS, McKhann GM, Sperling RA, Carrillo MC, et al. Introduction to the recommendations from the National Institute on Aging-Alzheimer's Association workgroups on diagnostic guidelines for Alzheimer's disease. Alzheimers Dement 2011;7:257–62.
[6] Minoshima S, Foster NL, Kuhl DE. Posterior cingulate cortex in Alzheimer's disease. Lancet 1994;344:895.
[7] Reiman EM, Caselli RJ, Yun LS, Chen K, Bandy D, Minoshima S, et al. Preclinical evidence of Alzheimer's disease in persons homozygous for the ε4 allele for apolipoprotein E. N Engl J Med 1996;334:752–8.
[8] Knopman DS, Jack CR, Wiste HJ, Lundt ES, Weigand SD, Vemuri P, et al. 18F-fluorodeoxyglucose positron emission tomography, aging, and apolipoprotein E genotype in cognitively normal persons. Neurobiol Aging 2014;35:2096–106.
[9] De Leon MJ, Convit A, Wolf OT, Tarshish CY, DeSanti S, Rusinek H, et al. Prediction of cognitive decline in normal elderly subjects with 2-

[(18)F]fluoro-2-deoxy-D-glucose/positron-emission tomography (FDG/PET). Proc Natl Acad Sci U S A 2001;98:10966–71.
[10] Scheef L, Spottke A, Daerr M, Joe A, Striepens N, Kölsch H, et al. Glucose metabolism, gray matter structure, and memory decline in subjective memory impairment. Neurology 2012;79:1332–9.
[11] Lowe VJ, Weigand SD, Senjem ML, Vemuri P, Jordan L, Kantarci K, et al. Association of hypometabolism and amyloid levels in aging, normal subjects. Neurology 2014;82:1959–67.
[12] Oh H, Habeck C, Madison C, Jagust W. Covarying alterations in Aβ deposition, glucose metabolism, and gray matter volume in cognitively normal elderly: Aβ, metabolism, gray matter volume, and aging. Hum Brain Mapp 2014;35:297–308.
[13] Yi D, Lee DY, Sohn BK, Choe YM, Seo EH, Byun MS, et al. Beta-amyloid associated differential effects of APOE ε4 on brain metabolism in cognitively normal elderly. Am J Geriatr Psychiatry 2014;22:961–70.
[14] Braak H, Braak E. Staging of Alzheimer's disease-related neurofibrillary changes. Neurobiol Aging 1995;16:271–8.
[15] Braak H, Thal DR, Ghebremedhin E, Del Tredici K. Stages of the pathologic process in Alzheimer disease: age categories from 1 to 100 years. J Neuropathol Exp Neurol 2011;70:960–9.
[16] Jack CR Jr, Knopman DS, Jagust WJ, Shaw LM, Aisen PS, Weiner MW, et al. Hypothetical model of dynamic biomarkers of the Alzheimer's pathological cascade. Lancet Neurol 2010;9:119–28.
[17] Pettigrew C, Soldan A, Moghekar A, Wang M-C, Gross AL, O'Brien R, et al. Relationship between cerebrospinal fluid biomarkers of Alzheimer's disease and cognition in cognitively normal older adults. Neuropsychologia 2015;78:63–72.
[18] Fischl B, Salat DH, Busa E, Albert M, Dieterich M, Haselgrove C, et al. Whole brain segmentation: automated labeling of neuroanatomical structures in the human brain. Neuron 2002;33:341–55.
[19] Fisher RA. On the "probable error" of a coefficient of correlation deduced from a small sample. Metron 1921;1:3–32.
[20] Soper D. Significance of the difference between two correlations calculator; 2015. Available at: http://www.danielsoper.com/statcalc. Accessed July 24, 2016.
[21] Fagan AM, Mintun MA, Shah AR, Aldea P, Roe CM, Mach RH, et al. Cerebrospinal fluid tau and ptau181 increase with cortical amyloid deposition in cognitively normal individuals: implications for future clinical trials of Alzheimer's disease. EMBO Mol Med 2009;1:371–80.
[22] Sperling RA, Aisen PS, Beckett LA, Bennett DA, Craft S, Fagan AM, et al. Toward defining the preclinical stages of Alzheimer's disease: recommendations from the National Institute on Aging-Alzheimer's Association workgroups on diagnostic guidelines for Alzheimer's disease. Alzheimers Dement 2011;7:280–92.
[23] Haier RJ, Alkire MT, White NS, Uncapher MR, Head E, Lott IT, et al. Temporal cortex hypermetabolism in Down syndrome prior to the onset of dementia. Neurology 2003;61:1673–9.
[24] Head E, Lott IT, Hof PR, Bouras C, Su JH, Kim R, et al. Parallel compensatory and pathological events associated with tau pathology in middle aged individuals with Down syndrome. J Neuropathol Exp Neurol 2003;62:917–26.
[25] Shaw LM, Vanderstichele H, Knapik-Czajka M, Figurski M, Coart E, Blennow K, et al. Qualification of the analytical and clinical performance of CSF biomarker analyses in ADNI. Acta Neuropathol 2011;121:597–609.
[26] Braak H, Braak E. Demonstration of amyloid deposits and neurofibrillary changes in whole brain sections. Brain Pathol 1991;1:213–6.
[27] Thal DR, Rüb U, Orantes M, Braak H. Phases of a beta-deposition in the human brain and its relevance for the development of AD. Neurology 2002;58:1791–800.
[28] Bien-Ly N, Andrews-Zwilling Y, Xu Q, Bernardo A, Wang C, Huang Y. C-terminal-truncated apolipoprotein (apo) E4 inefficiently clears amyloid-β (Aβ) and acts in concert with Aβ to elicit neuronal and behavioral deficits in mice. Proc Natl Acad Sci U S A 2011;108:4236–41.
[29] Dodart J-C, Marr RA, Koistinaho M, Gregersen BM, Malkani S, Verma IM, et al. Gene delivery of human apolipoprotein E alters brain Aβ burden in a mouse model of Alzheimer's disease. Proc Natl Acad Sci U S A 2005;102:1211–6.
[30] Andrews-Zwilling Y, Bien-Ly N, Xu Q, Li G, Bernardo A, Yoon SY, et al. Apolipoprotein E4 causes age- and tau-dependent impairment of GABAergic interneurons, leading to learning and memory deficits in mice. J Neurosci 2010;30:13707–17.
[31] Brecht WJ, Harris FM, Chang S, Tesseur I, Yu G-Q, Xu Q, et al. Neuron-specific apolipoprotein E4 proteolysis is associated with increased tau phosphorylation in brains of transgenic mice. J Neurosci 2004;24:2527–34.
[32] Hirai K, Aliev G, Nunomura A, Fujioka H, Russell RL, Atwood CS, et al. Mitochondrial abnormalities in Alzheimer's disease. J Neurosci 2001;21:3017–23.
[33] Dumanis SB, Tesoriero JA, Babus LW, Nguyen MT, Trotter JH, Ladu MJ, et al. ApoE4 decreases spine density and dendritic complexity in cortical neurons in vivo. J Neurosci 2009;29:15317–22.
[34] Huang Y. Roles of apolipoprotein E4 (ApoE4) in the pathogenesis of Alzheimer's disease: lessons from ApoE mouse models. Biochem Soc Trans 2011;39:924–32.
[35] Kok E, Haikonen S, Luoto T, Huhtala H, Goebeler S, Haapasalo H, et al. Apolipoprotein E–dependent accumulation of Alzheimer disease–related lesions begins in middle age. Ann Neurol 2009;65:650–7.
[36] Landau SM, Mintun MA, Joshi AD, Koeppe RA, Petersen RC, Aisen PS, et al. Amyloid deposition, hypometabolism, and longitudinal cognitive decline. Ann Neurol 2012;72:578–86.
[37] Knopman DS, Jack CR Jr, Wiste HJ, Weigand SD, Vemuri P, Lowe VJ, et al. Brain injury biomarkers are not dependent on β-amyloid in normal elderly. Ann Neurol 2013;73:472–80.
[38] Förster S, Grimmer T, Miederer I, Henriksen G, Yousefi BH, Graner P, et al. Regional expansion of hypometabolism in Alzheimer's disease follows amyloid deposition with temporal delay. Biol Psychiatry 2012;71:792–7.
[39] Edison P, Archer HA, Hinz R, Hammers A, Pavese N, Tai YF, et al. Amyloid, hypometabolism, and cognition in Alzheimer disease: an [11C]PIB and [18F]FDG PET study. Neurology 2007;68:501–8.
[40] Rosenbloom MH, Alkalay A, Agarwal N, Baker SL, O'Neil JP, Janabi M, et al. Distinct clinical and metabolic deficits in PCA and AD are not related to amyloid distribution. Neurology 2011;76:1789–96.
[41] Mosconi L, Andrews RD, Matthews DC. Comparing brain amyloid deposition, glucose metabolism, and atrophy in mild cognitive impairment with and without a family history of dementia. J Alzheimers Dis 2013;35:509–24.